ARTICLES

np elastic spin transfer measurements at 788 MeV

M. W. McNaughton, K. Koch, I. Supek, and N. Tanaka*
Los Alamos National Laboratory, Los Alamos, New Mexico 87545

K. H. McNaughton, P. J. Riley, D. A. Ambrose, J. D. Johnson, and A. Smith
University of Texas, Austin, Texas 78712

G. Glass, J. C. Hiebert, L. C. Northcliffe, and A. J. Simon
Texas A&M University, College Station, Texas 77843

D. L. Adams
Rice University, Houston, Texas 77251

R. D. Ransome and D. B. Clayton
Rutgers University, Piscataway, New Jersey 08854

H. M. Spinka
Argonne National Laboratory, Argonne, Illinois 60439

R. H. Jeppeson
University of Montana, Missoula, Montana 59812

G. E. Tripard
Washington State University, Pullman, Washington 99164
(Received 17 June 1991)

We have measured the spin-transfer parameters K_{LL}, K_{SL}, K_{LS}, and K_{SS} at 788 MeV from 47° to 177° c.m., and also uncovered a 10–16 % normalization discrepancy which affects all previous *np* elastic spin data from LAMPF. Results disagree significantly from previous phase-shift predictions. With the inclusion of these new data the *NN* phase shifts and amplitudes (isospin 0 and 1) become well determined for the first time near 800 MeV.

I. INTRODUCTION

A major goal at LAMPF has been to determine the nucleon-nucleon isospin-zero (NN $I=0$) phase shifts and amplitudes near 800 MeV. We have measured four spin-transfer observables which, when combined with previous spin-dependent data near 800 MeV, lead to stable solutions.

As recently as 1988 Arndt [1] stated that above 500 MeV the NN $I=0$ phase shifts were "essentially undefined." Bugg [2] pointed out that the spin-transfer observables K_{LL}, K_{SS}, and K_{NN} were needed to establish stable, well-determined solutions. Since our experimental method measures K_{LS} simultaneously with K_{LL} and K_{SL} simultaneously with K_{SS}, we have measured these four observables. This overdetermination allows some cross-checking of possible systematic errors as described below.

Previous spin-dependent data for *np* free scattering near 800 MeV are the analyzing powers [3–6] the four spin-correlation parameters [7–11], and spin-transfer parameters near 180° c.m. [12,13]. In addition, the spin-dependent total cross sections $\Delta\sigma_L$ and $\Delta\sigma_T$ [14–17] have recently been measured. Finally, the analyzing power [6] A_N and spin-depolarization parameters D_{ij} have been measured for the quasifree reaction from the neutron in deuterium [18]. (Note that the quoted uncertainties for A_N in Ref. [6] are statistical only.)

Experience with the isospin-1 (pp) system has shown that the phase-shift analysis becomes reliable only when there are sufficient data to overdetermine the five scattering amplitudes independently of theoretical input. With less data the phase-shift analysis relies more heavily on theoretical and phenomenological input to fix the higher partial waves. Furthermore, the data set may contain systematic errors which were unsuspected but which show up as internal inconsistencies once the amplitudes become overdetermined. Failure to account for these errors leads to overly optimistic estimates of the uncertain-

ties. Comparing the phase-shift predictions before inclusion of the present data with the latest fits we see changes of five standard deviations in K_{LL} near 125°, in K_{LS} near 100°, in K_{SL} near 155°, and in K_{SS} near 130°. A similar change was noted [19] when the *pp* data set became sufficient to overdetermine the $I=1$ amplitudes.

Spinka [20] has shown that one can solve for the amplitudes up to a discrete fourfold ambiguity using only the cross section, analyzing power, and the four spin-correlation parameters. The addition of two of the spin-transfer parameters reported here, K_{LL} and K_{LS}, completely determines the five complex scattering amplitudes. When K_{SS} and K_{SL} are included then the amplitudes are overdetermined for the first time.

Nucleon-nucleon databases and phase-shift analyses are maintained by Arndt [21], Bugg [2], Bystricky, Lehar, and Leluc [22], and Hoshizaki [23,24]. They reported that, with the inclusion of the new data reported here, the phase-shift analyses show "an immense improvement" and are well determined with well-behaved error matrices for the first time. Correlations in the error matrix have almost disappeared, and previously reported problems [2] near 800 MeV have disappeared. Bugg reports a χ^2 per point of 1.1 for his fits to the new data reported here.

II. EXPERIMENTAL METHOD

A. Proton beam

Polarized protons from the optically pumped source OPPIS were accelerated to 798 MeV in the LAMPF accelerator. A solenoid and bending magnets precessed the spin direction to $\pm L$ (parallel or antiparallel to the momentum). All components of the proton-beam polarization and spin direction were measured to ± 0.01 by two polarimeters separated by a 16° bend. The proton beam was focused to a spot with rms radius of about 3 mm and centered on the 25-cm-thick liquid-deuterium (LD2) neutron-production target.

B. Neutron beam

Longitudinally polarized (L-spin) neutrons near 0° were produced by the ^{2}H(p,n) reaction. The high-energy neutrons selected by the time-of-flight and momentum tests (Sec. II E) have a mean energy of 788 MeV and a rms width of 3 MeV.

The spin-transfer parameters for this reaction have been previously measured, and were remeasured in this experiment. (This is discussed in Sec. III.) Neutrons were collimated near 0° by a 3.6-m-long collimator through a 3.6-m steel wall. Collimators of various diameters were used. All were conical, pointing to a vertex at the neutron production (LD2) target, with half angles ranging from 3 mr (2.5 cm/757 cm) to 9 mr (7 cm/757 cm).

The L-to-L spin-transfer parameter from deuterium is large while the other spin-transfer parameters are small, so that the neutrons were initially polarized in the L direction, almost independent of the precise proton spin direction. Immediately after the neutron-production target, the proton beam was swept aside by two 15° bending magnets (LBBM6,7). The neutrons passed through the fringe fields of these magnets and were precessed about 50° from L spin. A vertical magnetic field (BRBM1) immediately after the collimator served several functions: (1) to precess the spin +50° back to exact L spin, (2) to precess the spin −40° to S spin (sideways [25]), and (3) to sweep charged particles produced in the collimator out of the neutron beam, into a 60-cm-thick lead shield wall.

BRBM1 was mapped over the 20 cm diameter of the neutron beam. The integral fields were measured to be 0.5% lower on the left and right edges and 0.4% higher at the top and bottom. Hysteresis was less than 0.4%, corresponding to 0.2° of precession.

C. Experiment layout

The experiment layout is illustrated in Fig. 1 and discussed in detail below.

1. Target

The polarized neutron beam was directed onto a 15-liter liquid-hydrogen (LH2) target consisting of a cylinder 15 cm long and 12 cm in radius, with hemispherical end windows of 12 cm radius for a total length of about 39 cm. The end windows were 0.4-mm-thick Mylar plastic. The LH2 was contained in an insulating vacuum with entrance and exit windows each of 0.4-mm-thick Mylar and Kevlar plastic. The vacuum chamber was contained in a protective tent with Mylar plastic entrance and exit windows 25 μm thick.

The total material intercepted by the beam and visible to the spectrometer consisted of 2.5-g/cm^2 liquid hydrogen and less than 0.2-g/cm^2 plastic. The background from this plastic was 1% or less.

2. Neutron detector

Neutrons that scattered to beam-right were detected by a position-sensitive neutron detector [26] consisting of 24

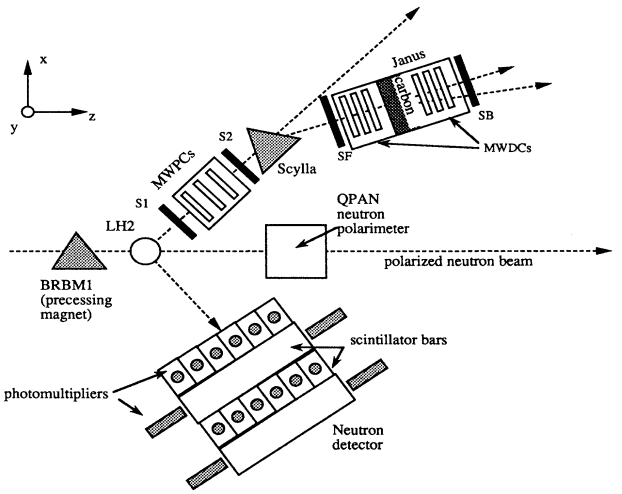

FIG. 1. Experimental layout.

slabs of plastic scintillator each 60 cm long by 11.4 cm wide by 25 cm deep. The 24 slabs were arranged in 4 banks of 6 slabs, alternately vertical (front and third bank) and horizontal (second and last bank). A photomultiplier was coupled to each end of each slab, so that the time difference between the ends measured the position of the hit.

All 48 photomultiplier signals went to time digitizers (TDC's), pulse-height digitizers (ADC's), and scalers, which were read via CAMAC into an on-line VAX computer where the position, angle, and time of the neutron hit was calculated. Angular resolution was typically a few degrees, depending on the scattering angle and detector distance, and was limited by the size of the LH2 target. Time resolution was better than 1 ns.

3. *Proton spectrometer*

Protons that scattered to beam-left were detected in the Scylla magnetic spectrometer. Two scintillators, S1 and S2, each 5 mm thick by 300 mm wide by 457 mm high, were placed upstream and downstream of a set of three multiwire proportional chambers (MWPC's M1, M2, M3) with 2-mm wire spacing and with active areas 320 mm wide by 512 mm high.

Two MWPC's defined the proton trajectory while the third MWPC provided redundant information as a check and to improve the overall efficiency at high rates. Individual amplifiers on every wire allowed the system to handle instantaneous singles rates up to about 1 MHz. M1 and M3 were 400 mm apart so that the proton scattering angle was measured with a resolution of ± 2.5 mrad. The chambers and the spectrometer were aligned with an absolute accuracy of about 1 mrad, so the uncertainty in the mean proton scattering angle was about $\pm 0.1°$ c.m. The scintillators measured the time relative to the accelerator rf to better than 1 ns.

After passing through S1, M1, M2, M3, and S2, the scattered proton trajectories were bent 30° in a vertical plane through Scylla, a bending magnet 1.22 m long with a gap 0.25 m wide by 0.56 m high. The Scylla magnet served two purposes: (1) to measure the proton momentum, and (2) to precess the final-state L-spin component through about 90° to allow this component to be measured by the Janus polarimeter. Momentum resolution was about 2%, limited by energy loss from the large LH2 target. The average spin precession in Scylla was deduced from the bend angle, which was measured to better than 0.2%.

4. *Janus polarimeter*

The Janus carbon polarimeter [27] (Fig. 1) consists of (1) a scintillator plane (SF) and multiwire drift chambers (MWDC's) to measure the proton time and trajectory; (2) a carbon analyzer, variable in thickness from 3 to 25 cm; and (3) MWDC's and a scintillator plane (SB) to measure the proton trajectory after scattering in the carbon. Janus has been used in LAMPF experiments 194, 403, 635, 636, 637, 708, 806, 807, 818, and 1035, and is well understood. It has been extensively calibrated [28,29] to 2% and its calibration agrees well with that of similar devices at Saturne [30], TRIUMF [31,32], and SIN/PSI [33].

The upstream Janus detectors complete the Scylla spectrometer by measuring the proton trajectory after bending and precessing in the Scylla magnet. From this we deduce the proton momentum and spin precession angle. The downstream Janus detectors measure the polar and azimuthal angles for the (inclusive) carbon scattering, from which we deduce two components of the final-state proton spin.

D. Spin transfer and notation

The final-state proton scattered from the LH2 target in general has three spin components: N, S, and L [25]. L is parallel to the momentum vector $\mathbf{k}$. N is vertical, normal to the scattering plane, defined as $\mathbf{k}_{\rm in}\times\mathbf{k}_{\rm out}$, where $\mathbf{k}_{\rm in}$ is the incident and $\mathbf{k}_{\rm out}$ is the outgoing momentum. S is defined by $N\times L$.

Several sign conventions are in common use. Bystricky, Lehar, and Winternitz [34] give explicit definitions, but their signs differ from Arndt's [21]. The notation and signs are summarized in Table I.

S spin is unaffected by the vertical bend in Scylla and is directly measured by down-up scattering in the Janus polarimeter, e.g., the polarization measured by Janus: $P=P_nK_{SS}$, where P_n is the neutron beam polarization. L and N spins are precessed in Scylla so that left-right scattering in Janus measures $P_+=P_nK_{LL}\sin\theta+A_{0N}\cos\theta$, where A_{0N} is the polarizing power and θ, the precession angle in Scylla, is near 90°. The beam polarization was flipped 180° at the ion source every 30 s thus changing the sign of the first term. Taking the difference $P_+-P_-=2P_nK_{LL}\sin\theta$ thus eliminates the second term. Similarly instrumental asymmetries (which are constant and do not change sign) are subtracted out.

E. Good events

Good events were selected in two categories, with and without the neutron detector. Data with the neutron detector in coincidence has less background but had larger statistical uncertainties. Final data were obtained from events without the neutron detector, but with a small correction for background as discussed in Sec. II F.

Good events were selected with the following tests.

1. *Incident time of flight: S12T*

S12T was the time of flight from the LD2 neutron production target to the mean of S1 and S2. The LAMPF

TABLE I. Sign convention and notation.

This work	Arndt	Bystricky
K_{LS}	AT	$-K_{0sk0}$
K_{LL}	APT	$+K_{0kk0}$
K_{SS}	RT	$+K_{0ss0}$
K_{SL}	RPT	$-K_{0ks0}$

polarized beam was bunched at 10 MHz into bursts <1 ns wide, phased to the 10-MHz rf signal. The time was measured between the 10-MHz signal and the mean time of S1 and S2. This was primarily a measure of the incident neutron time of flight over the 12.5-m flight path from the LD2 to LH2 target, with the small addition of the proton flight time over the 2-m flight path from LH2 to S1 and S2. The measured time was corrected for the <1-ns kinematic variation over the angular acceptance. The typical resolution was ± 0.6 ns. Almost all low-energy neutrons produced by inelastic reactions in the LD2 neutron-production target were eliminated by this test.

2. *Scattered time of flight*

The time of flight was measured from the mean of S1 and S2 to SF, the front (upstream) Janus scintillator, and corrected for the <1-ns kinematic variation over the angular acceptance. The flight path was 2.5 m and the typical resolution was ± 0.7 ns. A test of this time of flight in conjunction with the momentum measurement (Sec. II E 7) selected proton events that were elastically scattered from the LH2 target.

3. *Good MWPC's*

The redundant information in three wire chambers was used to correct events in which a chamber fired twice within the 100-ns gate. The three-chamber hits were required to lie on a straight line with no more than 2-mm deviation.

4. *Good trajectories*

The proton trajectory was required to trace back to the LH2 target. The trajectories from the wire chambers on either side of the Scylla magnet were required to meet at the center of Scylla, typically within 2 or 3 cm, and the X bend (parallel to the magnetic field) was required to be $0°\pm 2°$ (the Y bend measures the momentum; see momentum test below).

5. *Good Janus chambers*

The redundant information in three drift chambers was used to correct events in which a wire or a sign of the drift time was incorrect. The three chambers were required to define a straight line with no more than 1 mm deviation.

6. *Good Janus tests*

The standard Janus tests [27] were applied. These are the two trajectories intersect in the carbon within 5 mm of each other, unbiased acceptance for both azimuthal angle ϕ and opposite angle $\phi+\pi$, and polar scattering angle greater than the multiple Coulomb scattering angle (3° to 6° depending on the energy).

7. *Momentum*

The Scylla spectrometer measured the proton momentum typically with 2% resolution, limited by energy loss in the large LH2 target. Background from the target walls was less than about 1% for data without the neutron detector, and less than 0.2% for the data that included the neutron detector. Typical momentum spectra are shown in Fig. 2.

F. Background

Background was monitored two different ways. First, asymmetries were measured for events in the wings of the momentum spectrum. Typically these asymmetries were 0.5 to 1.0 times the asymmetry in the elastic peak. Background under the peak [Fig. 2(a)] was estimated to be about 1% indicating background corrections of less than about 0.5%.

Second, we calculated the ratio of the asymmetries with and without the neutron detector in coincidence. The average ratio was 1.004 ± 0.008. The ratio is statistically significant only when the magnitude of the asymmetry is large, so this result is dominated by K_{LL} near 25° laboratory angle.

Detailed examination of individual cases resulted in background corrections of -0.004 to K_{LL} from 22° to

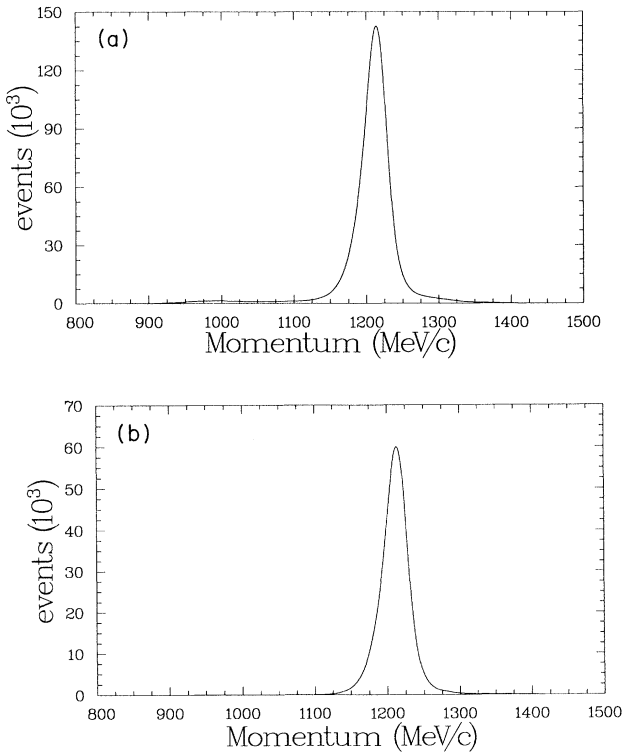

FIG. 2. Momentum histogram showing the elastic peak and the low-momentum tail, (a) without the neutron detector and (b) with the neutron detector in coincidence. (Bins are 10 MeV/c wide; individual points are connected with a smooth curve.)

32° laboratory and -0.002 to K_{LL} near 20° laboratory angle. The uncertainty in the background correction is estimated to be ± 0.002, which is negligible compared with the other uncertainties. All other cases would have corrections of ± 0.001 or less, and so were not corrected for background.

G. Azimuthal scattering angle

Near 0° laboratory angle (180° c.m.) there is a significant dependence on the azimuthal angle ϕ_p of the *np* elastic scattering. At 174.7° and 177.4° c.m. the data were binned into eight ϕ_p bins and fit to appropriate azimuthal distribution. The $\cos\phi$ correction factors for K_{SL} and K_{LS} resulted in changes of <0.001 and so were neglected. For K_{SS} at 170.0°, 168.1°, 165.1°, and 158.2° c.m., the correction terms $K_{NN}\sin^2\phi_p$ were 0.59×0.036, 0.65×0.025, 0.63×0.013, and 0.4×0.006, respectively.

H. Spin direction

The spin direction of the polarized neutron beam from the LAMPF LD2 target has been examined in detail by Spinka [35]. This experiment used the same system except for a larger-diameter collimator and a larger-aperture magnet (BRBM1) after the collimator. Relocation of some beam-line components over the years may have resulted in small changes in alignment. Also it should be noted that in previous experiments it was standard practice to place about 5 radiation lengths (30 mm) of lead in the neutron beam to attenuate the gamma-ray flux; no lead was used in this experiment. We believe that these changes were all insignificant.

All three components (S, N, L) of the proton beam are measured by two beam-line polarimeters separated by a bend; the neutron spin direction after the ^{2}H(p,n) reaction in the LD2 target can be calculated from the ratio of the spin-transfer coefficients K_{LL}/K_{SS}. The proton beam is swept aside by the beam-line magnets LBBM6,7 (see Fig. 1 of Ref. [36] or Fig. 3 of Ref. [37]); the neutron beam (at 0°) passes through part of LBBM6,7 and is thus precessed by about 50°. The neutron precession magnet (BRBM1) is set either to restore the spin to L (canceling the precession in LBBM6,7) or to precess an additional 40° to give S spin.

The neutron spin direction is measured by a high-count-rate polarimeter, QPAN (similar to earlier versions [38,39]). QPAN measures the asymmetry of the protons scattered near 30° laboratory angle from the liquid-hydrogen target. The asymmetry is zero with an L-spin neutron beam and has a maximum with an S-spin neutron beam.

It is possible to compare our results with previous results [35] via the neutron precession in LBBM6,7. Our data imply a neutron precession of $53.4°\pm 0.2°$ in LBBM6,7; previous data implied $48°\pm 3°$. At the time this was reasonably close to the value of 49° expected from the field map of a similar magnet LBBM5, but recently it was discovered that the fringe field of the next beam-line magnet, LBBM7, causes an additional 5° of precession for a total of 54°. A recent analysis of the old data gave $49°\pm 3°$ for all energies combined and 53° for 788 MeV only.

Further indication that the previous value may be low comes from the field map of the old precession magnet (Lorraine, Ref. [35], Sec. D). If we assume that the Lorraine field map is correct then the older data imply a precession of 52° in LBBM6,7.

An anomalous observation occurred when QPAN was placed near 20° (because there was no available space at its location at 0°). In principle, if the beam spin is precisely parallel to the beam momentum (L spin) then the asymmetry must be zero regardless of the angle, but we observed a nonzero asymmetry of 0.007 ± 0.001. In the absence of systematic errors this would seem to indicate an S component, but this contradicted many runs with QPAN at 0° and asymmetries of 0.000 ± 0.001. Later attempts to reproduce and understand this anomaly with QPAN near 20° gave inconsistent results ranging from 0.003 ± 0.001 to 0.000 ± 0.001 (compared with asymmetries of 0.052 to 0.090 for S spin). We have no satisfactory explanation for this anomaly.

As a result of these possible discrepancies, we carried out a detailed search for systematic errors in the spin direction as described below.

Proton-beam steering could affect the neutron trajectory and thus the neutron precession. Steering the proton beam horizontally by 5 mm changed the spin direction (as measured by QPAN) by $1.0°\pm 0.3°$. This change is consistent with the field maps of LBBM6. Since the proton-beam steering is typically stable to ± 1 mm, we conclude that this effect is about $\pm 0.2°$.

Our large-diameter collimator might have an effect, e.g., if the neutron spin direction varies nonlinearly as a function of position. We repeated the most sensitive data (K_{SL} near 120°) with large (14 cm) and small (5 cm) collimators and concluded that the difference is smaller than 1.7°.

The neutron beam has a spectrum of energies including a high-energy peak and a tail of lower-energy neutrons [36,37] which precess differently in LBBM6,7 and BRBM1. The neutron polarimeter QPAN is designed to be insensitive to the lower-energy neutrons. Nevertheless, we searched for such a possibility by changing the QPAN parameters that affect its sensitivity to low-energy neutrons, and found no significant change.

For L-spin neutrons the precessions due to BRBM1 and LBBM6,7 cancel, so the presence of lower-energy neutrons would cause systematic errors only for S-spin neutrons. Therefore the neutrons are set to L-spin with high precision and without significant systematic error. To set to S spin either we can measure the QPAN asymmetry as a function of the BRBM1 setting and find the maximum or we can use the BRBM1 field measurements to calculate the change from the L to the S setting. These two methods agree to 0.6%; therefore we conclude that the possible systematic error is less than 0.5°.

Finally, we checked the neutron-beam spin direction using the relation [34]

$$(K_{LS}+K_{SL})/(K_{LL}-K_{SS})=\pm\tan\theta_{\rm lab}\ .$$

(The + or − sign depends on the sign convention as summarized in Table I.) The dominant effect of an incorrect spin direction would be to mix K_{LL} (which is large) into K_{SL} (which is small) so that the above relation would not hold. We derived the spin direction that would make the relation precisely true at each scattering angle. Averaging all the data, we calculated the optimum beam spin direction to be 0.5°±0.7° from our measured value, i.e., this check confirms our measurements to 0.7°.

We conclude that the uncertainty in spin direction generally makes a negligible contribution to the final uncertainty of the observables, except for K_{SL} near 120° c.m., where we have added 0.01 (in quadrature) to the uncertainties, corresponding to a 0.7°, uncertainty in the spin direction.

III. NORMALIZATION

The polarization of the primary proton beam is measured by two beam-line polarimeters (separated by a bend to measure all three spin components). The beam-line polarimeters have been calibrated to 1% for a well-focused beam spot [40]. Experience has shown that with a poorly focused beam the uncertainty increases to 2% as a result of increased contamination by quasifree scattering from carbon in the CH2 targets. (We used the conservative value of 0.473±0.010 for the polarimeter analyzing power.)

To deduce the polarization of the neutron beam we need the spin-transfer coefficient $K_{LL}(d)$ for the neutron production reaction ^{2}H(p,n). By charge symmetry this

TABLE II. Spin-transfer observables for *np* elastic scattering at 788 MeV. The overall normalization uncertainty is 2.4%.

$\theta_{c.m.}$ (deg)	θ_{lab} (deg)	K_{LS}	K_{LL}	K_{SS}	K_{SL}
177.4	1.08	−0.019±0.039	−0.570±0.027	−0.046±0.046	−0.038±0.039
174.7	2.23	−0.002±0.052	−0.444±0.033	−0.181±0.063	0.075±0.049
170.0	4.21	−0.009±0.044	−0.284±0.045	−0.574±0.047	0.042±0.047
168.1	5.01	0.024±0.042	−0.312±0.043	−0.717±0.048	0.044±0.047
165.1	6.94	−0.063±0.051	−0.284±0.052	−0.592±0.057	−0.026±0.057
158.2	9.20	−0.093±0.037	−0.386±0.038	−0.431±0.047	0.117±0.047
156.6	9.87	−0.039±0.039	−0.407±0.040	−0.341±0.050	−0.003±0.049
154.7	10.66	−0.114±0.032	−0.508±0.034	−0.393±0.040	0.024±0.040
146.6	14.13	−0.190±0.042	−0.602±0.043	−0.013±0.042	0.017±0.043
144.9	14.86	−0.195±0.048	−0.688±0.050	−0.020±0.048	0.064±0.050
143.0	15.67	−0.146±0.039	−0.747±0.042	−0.077±0.040	0.029±0.041
136.0	18.72	−0.303±0.038	−0.810±0.041	0.110±0.034	−0.091±0.035
133.4	19.85	−0.289±0.035	−0.789±0.038	0.160±0.031	−0.078±0.032
130.5	21.13	−0.296±0.030	−0.892±0.034	0.181±0.031	−0.107±0.033
125.8	23.24	−0.309±0.030	−0.873±0.033	0.092±0.029	−0.174±0.031
122.5	24.73	−0.400±0.037	−0.906±0.040	0.081±0.025	−0.103±0.027
119.0	26.30	−0.249±0.036	−0.974±0.041	0.084±0.024	−0.141±0.027
114.3	28.46	−0.358±0.037	−0.791±0.039	−0.012±0.045	−0.151±0.046
110.8	30.07	−0.319±0.024	−0.724±0.028	−0.043±0.030	−0.087±0.031
107.3	31.70	−0.362±0.035	−0.773±0.037	−0.013±0.041	−0.025±0.042
103.7	33.40	−0.348±0.033	−0.638±0.035	−0.059±0.035	−0.005±0.037
100.6	34.86	−0.393±0.033	−0.569±0.035	0.008±0.035	0.015±0.037
97.3	36.47	−0.409±0.029	−0.536±0.030	−0.005±0.028	0.042±0.029
92.9	38.58	−0.451±0.027	−0.462±0.028	−0.077±0.028	0.078±0.029
89.8	40.11	−0.391±0.029	−0.443±0.030	−0.001±0.030	0.145±0.031
86.6	41.67	−0.367±0.025	−0.382±0.025	−0.092±0.026	0.142±0.027
83.1	43.42	−0.333±0.040	−0.334±0.042	−0.040±0.035	0.206±0.037
79.9	45.04	−0.326±0.028	−0.247±0.029	−0.075±0.026	0.106±0.027
76.7	46.70	−0.166±0.032	−0.156±0.033	−0.036±0.028	0.093±0.029
73.3	48.42	−0.188±0.038	−0.236±0.040	−0.051±0.036	0.106±0.040
70.0	50.18	−0.094±0.028	−0.049±0.030	−0.084±0.028	0.091±0.030
65.4	52.61	−0.023±0.030	−0.051±0.032	−0.061±0.028	0.035±0.031
63.6	53.54	−0.030±0.043	0.010±0.046	−0.005±0.045	0.056±0.050
60.7	55.10	−0.025±0.033	−0.012±0.036	−0.059±0.036	−0.015±0.039
57.5	56.83	−0.024±0.047	0.025±0.050	−0.064±0.050	−0.051±0.053
54.2	58.63	0.080±0.053	−0.023±0.060	−0.110±0.058	0.010±0.064
51.3	60.20	0.072±0.057	−0.014±0.060	−0.115±0.064	0.073±0.065
49.3	61.34	0.089±0.057	0.057±0.058	0.037±0.057	−0.028±0.064
46.8	62.71	0.190±0.095	0.080±0.085	0.044±0.088	0.012±0.097

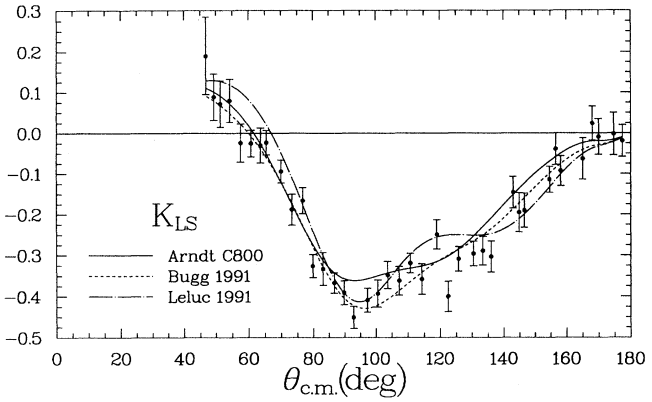

FIG. 3. Spin-transfer observable K_{LS} at 788 MeV compared with recent phase shift fits by Arndt, Bugg, and Leluc.

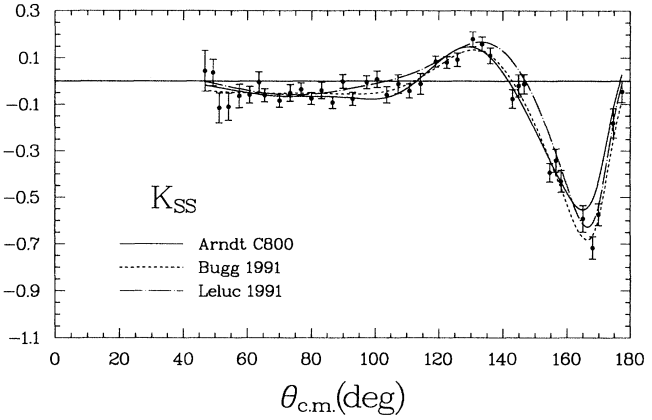

FIG. 5. Spin-transfer observable K_{SS} at 788 MeV compared with recent phase-shift fits by Arndt, Bugg, and Leluc.

should be equal to $K'_{LL}(d)$ for ^{2}H(n,p). We measured these by placing the Scylla+Janus spectrometer at 0° and filling the second target with liquid deuterium. If P_b is the proton-beam polarization then the neutron-beam polarization is $P_b K_{LL}(d)$ and the protons scattered into the spectrometer have a polarization of

$$P_b K_{LL}(d) K'_{LL}(d) = P_b (K_{LL})^2$$

if $K_{LL} = K'_{LL}$. Using the Janus polarimeter to measure this polarization we deduced $K_{LL}(d)$.

Possible systematic errors in this technique are the assumption of charge symmetry, the 2.2-MeV energy change between the first and second scatters ($<0.1\%$ change in K_{LL}), background (0.002 correction), momentum acceptance (± 45 MeV/c), angular acceptance, proton-beam calibration, and Janus calibration. Only the last three are significant.

Averaged over the spectrometer acceptance (3°) we measure $K_{LL}(d) = -0.694$. As expected, however, we observe an angular dependence. Fitting the best parabola to the observed angular dependence we extrapolate a value of $K_{LL}(d) = -0.717$ at 0°. If we use the shape of K_{LL} for free *np* scattering then we obtain $K_{LL}(d) = -0.719$ at 0°. According to calculations by Bugg and Wilkin [41]. K_{LL} has an angular dependence of the form $K = K_0 - 0.018\theta^2_{\text{lab}}$. Using this function we get $K_{LL}(d) = -0.720$ at 0°. Integrating over the diameter of the largest neutron collimator used in these measurements (half angle $= 0.5°$) the average is -0.719.

As stated above, the proton-beam polarization and the Janus analyzing power have both been calibrated to 2% and agree with calibrations from TRIUMF [31,32], SIN/PSI [33], and Saturne [30]. As a test, we substituted the Saturne calibration [30] of the "POMME" carbon polarimeter for our standard calibration [29] for the Janus carbon polarimeter; this gave a value of $K_{LL}(d) = -0.726$, in good agreement with our value of -0.720.

Since we measure the square $K_{LL}(d)^2$, uncertainties are halved when we take the square root. Thus the 2% uncertainties in the analyzing powers of the beam-line polarimeter and the Janus polarimeter each become 1% for

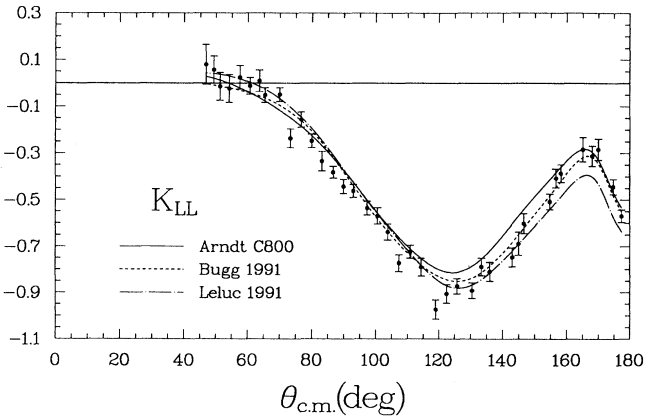

FIG. 4. Spin-transfer observable K_{LL} at 788 MeV compared with recent phase-shift fits by Arndt, Bugg, and Leluc.

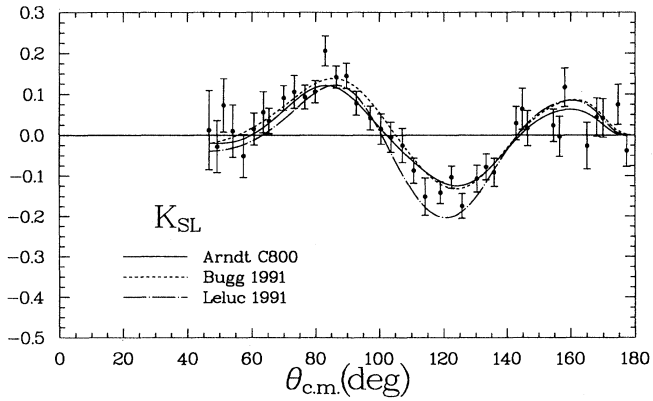

FIG. 6. Spin-transfer observable K_{SL} at 788 MeV compared with recent phase-shift fits by Arndt, Bugg, and Leluc.

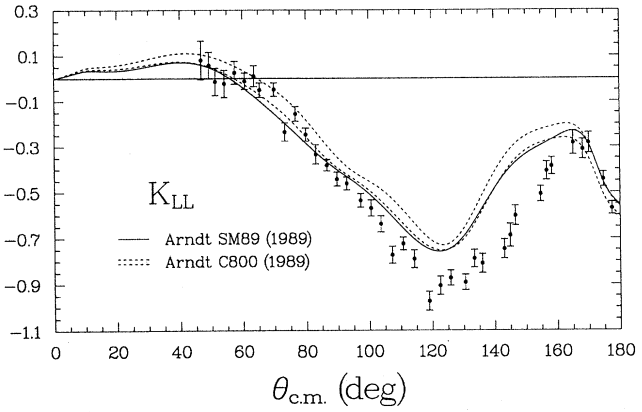

FIG. 7. Spin-transfer observable K_{LL} at 788 MeV compared with Arndt's phase-shift predictions: C800 (single energy) and SM89 (energy dependent). The pair of dashed lines shows the error corridor for the C800 solution.

a total systematic uncertainty of 1.4% or ±0.010. Combining this with the statistical uncertainty of ±0.014 we get $K_{LL}(d) = -0.720 \pm 0.017$ for small ($<0.3°$) collimators and -0.719 ± 0.017 for the largest (0.5°) collimator.

This result disagrees with the previous results. Riley *et al.* [42] measured $K_{LL}(d) = -0.64 \pm 0.014$; Chalmers *et al.* [43] measured $K_{LL}(d) = -0.604 \pm 0.016$; these uncertainties are statistical only. However, both these measurements share a common systematic uncertainty of 7% from the *np* elastic analyzing power to which both of these results were normalized. Riley *et al.* normalized directly to the analyzing power data of Newsom *et al.* [3], which has 7% normalization uncertainty. (Riley *et al.* quote 4% in their paper, but this was revised to 7% in the final paper of Newsom *et al.*) Chalmers *et al.* normalized to a fit to the world data set [44], and also estimate 7% systematic uncertainty.

The disagreement with these earlier data suggests that the *np* elastic analyzing power data [3] should be renormalized, e.g., multiplying by (0.64/0.72). Bugg [2] and Bandyopadhyay *et al.* [45] have independently made the same suggestion. Since Newsom *et al.* [3] used a white neutron beam to measure from 375 to 775 MeV simultaneously, the suggested renormalization factor should take account of our recent LAMPF measurements of $K_{LL}(d)$ at 485 and 635 MeV. Preliminary results at these other energies suggest multiplying Newsom's data by 0.90.

Systematic errors from the beam polarization and carbon analyzing power enter into both the measurements of $K_{LL}(d)$ for ^{2}H(p,n) and K_{ij} for *np* elastic. These are correlated and partially cancel as follows. If J_1 and J_2 are the raw Janus asymmetries, A_C is the carbon analyzing power, P_b is the proton beam polarization, and P_n is the neutron beam polarization, then $K_{LL}(d) = \sqrt{J_1}/(\sqrt{A_C}\sqrt{P_b})$ and $K_{ij} = J_2/(A_C P_n)$. But $P_n = P_b K_{LL}(d)$ so $K_{ij} = J_2/(\sqrt{J_1}\sqrt{A_C}\sqrt{P_b})$. Therefore the overall normalization uncertainty of K_{ij} is equal to the relative uncertainty of $K_{LL}(d)$: 0.017/0.720=2.4%. There is an energy dependence to A_C but this has already been included as a point-to-point uncertainty in Table II. So, in summary, the overall normalization uncertainty, to be applied equally to all the data in Table II, is 2.4%.

IV. RENORMALIZATION OF PREVIOUS DATA

Based on the above calibration of $K_{LL}(d) = -0.720 \pm 0.017$, we recommend renormalizing several previous data sets near 790 MeV as follows. Ransome *et al.* [12] multiply by 0.64/0.72. Nath *et al.* [11] and Glass *et al.* [44] multiply by 0.604/0.720. The data of Rawool, Garnett *et al.* [7–10], and Beddo [14,15] extend over several energies and were all normalized to Chalmers *et al.* [43]. Our forthcoming paper on the recent $K_{LL}(d)$ measurements will include suggested renormalization factors at these other energies.

V. RESULTS

Four spin-transfer observables have been measured for 788-MeV polarized neutrons incident on liquid hydrogen, measuring the spin transfer to the outgoing proton. The observables are defined in Table I and listed in Table II. The overall normalization uncertainty is 2.4%.

In Figs. 3–6 the data are compared with new phase-shift solutions by Arndt, Bugg [46], Leluc, and Lehar, which include our new data and recommended renormalizations; Fig. 7 shows previous predictions. These authors report that with the inclusion of these new data the solutions are well determined with a well-behaved error matrix for the first time near 800 MeV.

ACKNOWLEDGMENTS

We are grateful to David Bugg, Dick Arndt, Jiri Bystricky, Franz Lehar, and Catherine Leluc for many helpful discussions and suggestions. One of us (M.W.M.) first heard the method for recalibrating $K_{LL}(d)$ from David Bugg. We also thank Dave Lopiano, Dan Allcock, Steve Means, and Zain Mujtaba for assistance during the setup and data taking. This work is supported in part by the U.S. Department of Energy Contract No. W-7405-ENG-36, Grants No. DE-FG05-88ER40446 and DE-FG05-88ER40399, and by the National Science Foundation.

*Deceased.

[1] R. A. Arndt Phys. Rev. D **37**, 2665 (1988).
[2] D. V. Bugg, Phys. Rev. C **41**, 2708 (1990).
[3] C. R. Newsom *et al.*, Phys. Rev. C **39**, 965 (1989).
[4] G. Glass *et al.*, Phys. Rev. C **41**, 2732 (1990).
[5] A. de Lesquen *et al.*, Nucl. Phys. **B304**, 673 (1988).
[6] M. Barlett *et al.*, Phys. Rev. C **27**, 682 (1983).
[7] G. R. Burleson *et al.*, Phys. Rev. Lett. **59**, 1645 (1987).
[8] R. Garnett *et al.*, Phys. Rev. D **40**, 1708 (1989).
[9] M. W. Rawool, NMSU thesis and Los Alamos Report LA-11387-T, 1988.
[10] R. W. Garnett, NMSU thesis and Los Alamos Report

LA-11491-T, 1989.
[11] S. Nath *et al.*, Phys. Rev. D **39**, 3520 (1989).
[12] R. D. Ransome *et al.*, Phys. Rev. Lett. **48**, 781 (1982).
[13] R. D. Ransome, University of Texas thesis and Los Alamos Report LA-8919-T, 1981.
[14] M. E. Beddo, NMSU thesis and Los Alamos Report LA-11905-T, 1990.
[15] M. E. Beddo *et al.*, Phys. Lett. **258D**, 24 (1991).
[16] Y. Terrien *et al.*, Nucl. Phys. **A478**, 533 (1988).
[17] F. Lehar *et al.*, Phys. Lett. B **189**, 241 (1987).
[18] M. Barlett *et al.*, Phys. Rev. C **32**, 239 (1985); **40**, 2697 (1989).
[19] M. W. McNaughton *et al.*, in *Polarization Phenomena in Nuclear Physics—1980,* Proceedings of the Fifth International Symposium, Santa Fe, edited by G. G. Ohlson, R. E. Brown, N. Jarmie, W. W. McNaughton, and G. M. Hale, AIP Conf. Proc. No. 69 (AIP, New York, 1981), p. 149.
[20] H. Spinka, Phys. Rev. D **30**, 1461 (1984).
[21] R. A. Arndt, Phys. Rev. D **35**, 128 (1987).
[22] J. Bystricky, C. Lechanoine-Leluc, and F. Lehar, J. Phys. (Paris) **48**, 199 (1987); **51**, 2747 (1990).
[23] N. Hoshizaki, Prog. Theor. Phys. **60**, 1796 (1978).
[24] N. Hoshizaki *et al.*, in Proceedings of the Workshop on Polarized Proton and Electron Beams (KEK, Ibaraki, Japan, 1988).
[25] *Higher Energy Polarized Proton Beams,* Proceedings of the Workshop, Ann Arbor, 1977, edited by A. D. Krisch and A. J. Salthouse, AIP Conf. Proc. Proc. No. 42 (AIP, New York, 1978), p. 142.
[26] R. Garnett *et al.*, Nucl. Instrum. Methods (to be published).
[27] R. D. Ransome *et al.*, Nucl. Instrum. Methods **201**, 309 (1982).
[28] R. D. Ransome *et al.*, Nucl. Instrum. Methods **201**, 315 (1982).
[29] M. W. McNaughton *et al.*, Nucl. Instrum. Methods **A241**, 435 (1985).
[30] B. Bonin *et al.*, Nucl. Instrum. Methods **A288**, 379 (1990).
[31] G. Waters *et al.*, Nucl. Instrum. Methods **153**, 401 (1978).
[32] O. Hausser *et al.*, Nucl. Instrum. Methods **A254**, 67 (1987).
[33] E. Aprile-Giboni *et al.*, Nucl. Instrum. Methods **215**, 147 (1983).
[34] J. Bystricky, F. Lehar, and P. Winternitz, J. Phys. (Paris) **39**, 1 (1978).
[35] H. Spinka, Argonne National Laboratory Report ANL-HEP-TR-88-14, 1988.
[36] C. W. Bjork *et al.*, Phys. Lett. **63B**, 31 (1976).
[37] C. W. Bjork, University of Texas thesis and Los Alamos Report LA-6192-T, 1976.
[38] C. L. Hollas *et al.*, Nucl. Instrum. Methods **A219**, 275 (1984).
[39] C. L. Hollas *et al.*, in *Polarization Phenomena in Nucleon Physics—1980* [19], p. 949.
[40] M. W. McNaughton *et al.*, Phys. Rev. C **24**, 1778 (1981).
[41] D. V. Bugg and C. Wilkin, Nucl. Phys. **A467**, 575 (1987).
[42] P. J. Riley *et al.*, Phys. Lett. **103B**, 313 (1981).
[43] J. S. Chalmers *et al.*, Phys. Lett. **153B**, 235 (1985).
[44] H. Spinka, Report ANL-HEP-TR-85-35, 1985.
[45] D. Bandyopadhyay *et al.*, Phys. Rev. C **40**, 2684 (1989).
[46] D. V. Bugg and R. A. Bryan, Nucl. Phys. A (submitted).